# Ground instability detection using PS-InSARin Lanzhou, China

Zeng, R. Q. [a], Meng, X. M. [a,*], Wasowski, J.[b], Dijkstra, T.[c], Bovenga, F.[d], Xue, Y. T.[a], Wang, S. Y.[a]

[a] MOE Key Laboratory of Western China's Environmental Systems, Lanzhou University, Lanzhou, Gansu, 730000, China

[b] CNR-IRPI, via Amendola 122 I, 70126 Bari, Italy

[c] British Geological Survey, Environmental Science Centre,Keyworth, Nottingham,NG12 5GG,United Kingdom

[d] CNR-ISSIA, via Amendola 122 D, 70126 Bari, Italy

* Corresponding author. TEL: +86-931-8912880; FAX: +86-931-8912330; E-mail: xmmeng@lzu.edu.cn (Meng, X.M.)

**Abstract:** This paper reports on the application of radar satellite data and Persistent Scatterer Interferometry (PS-InSAR) techniques for the detection of ground deformation in the semi-arid loess region of Lanzhou, northwestern China. Compared to Synthetic Aperture Radar Interferometry (In-SAR), PS-InSAR overcomes the problems of temporal and geometrical de-correlation and atmospheric heterogeneities by identifying persistent radar targets (PS) in a series of interferograms. The SPINUA algorithm was used to process 40 ENVISAT ASAR images for the target period 2003-2010. The analysis resulted in the identification of over 140,000 PS in the greater Lanzhou area covering some 300 km$^2$. The spatial distribution of moving radar targets was checked during a field campaign and highlights the range of ground instability problems that the Lanzhou area faces as urban expansion continues to accelerate. The PS-InSAR application detected ground deformations with rates up to 10 mm/year; it resulted in the detection of previously unknown unstable slopes and two areas of subsidence.

**Keywords: Loess slope, Geohazard, PS-InSAR, Ground instability, Lanzhou**

## 1 Introduction

Lanzhou is the capital of Gansu Province and is one of the most important industrial cities in northwest China (Figure 1). The 12th Five-Year plan and the 2011 National Economic and Social Development Statistical Bulletin of Lanzhou City indicate that the gross domestic product (GDP) of Lanzhou more than doubled in the last decade, reaching some 136 billion Yuan (approximately £13.6 billion). This is associated with a rapid increase in the urban population and current forecasts suggest that the remaining undeveloped land can only sustain further development for some 10 to 15 years (Yao 2008). Increasingly, people have to encroach on marginal areas having a greater potential for ground instability. Since 1949, a variety of geohazards (mainly comprising landslides, debris flows, soil collapse, subsidence and floods) in Lanzhou caused some 676 deaths and an estimated cumulative direct economic lossof some 756 million Yuan (Ding & Li 2009; Dijkstra *et al*., 2014). It is expected that further casualties and economic impacts will result in this unstable landscape unlessa better understanding of the spatial distribution and causes of typical geohazards involving ground instability can be implemented in the development of land use management practices, urban planning and the design of mitigation strategies. Satellite-based radar interferometry provides an opportunity to map ground deformation over large areas of interest. This paper highlights the use of PS-InSAR (Permanent Scatterer Synthetic Aperture Radar Interferometry) in a region where an incomplete ground instability inventory exists.

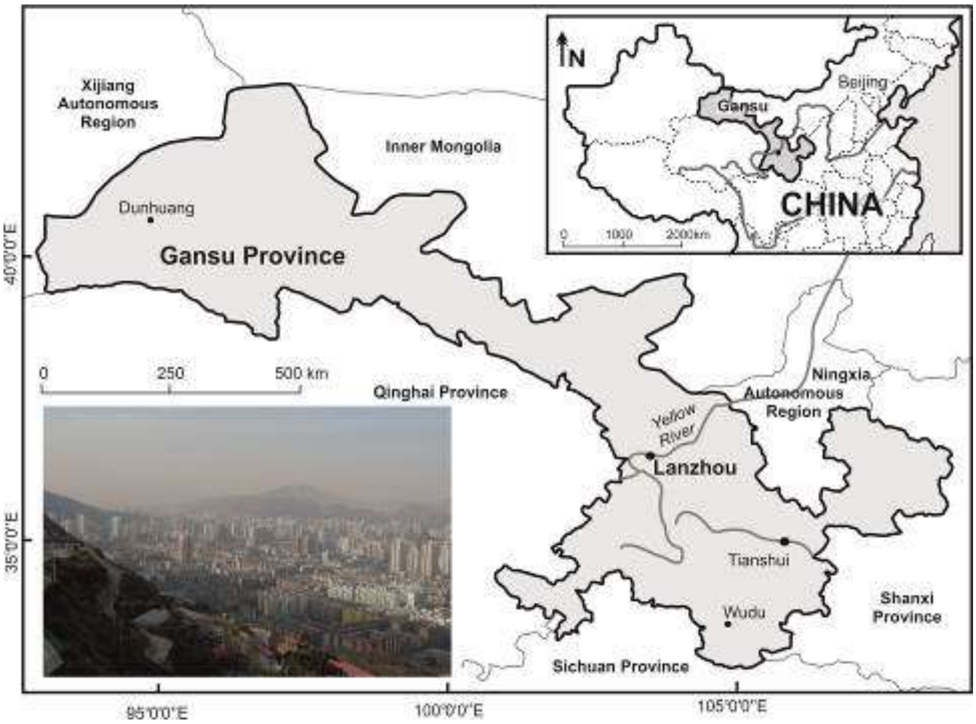


**Figure 1.** Location of Gansu Province and its capital Lanzhou. The photo shows the central urban area of Lanzhou and is looking towards the northwest with Jiuzhoutai Mountain in the centre (loess thickness more than 300m).

## 2 The study area

The city of Lanzhou is located on a series of river terraces of the Yellow River (*Huang He*), confined within a narrow structural basin with an east-west alignment (Figures 1, 2). To the north and south are mountainous regions characterised by a high relative relief, steep slopes and narrow valleys. Loess, a wind-blown cemented silt, covers most of this region with some deposits reaching thicknesses exceeding 300 m and with thicknesses greater than 50 m quite common (see Derbyshire *et al.,*. 2000 for a detailed account of landslide processes in these thick loess deposits). Lanzhou is positioned in an active neo-tectonic region forming the northeast extension zone of the Tibetan Plateau (Dijkstra *et al*., 1993; Li *et al*., 1993; Derbyshire *et al*., 2000). Frequent earthquakes are driven by stress release along a family of strike-slip faults with four major fault systems recognised in the Lanzhou region, the Jinchengguan Fault, Leitanhe Fault, Si'ergou Fault and Xijincun Fault (Yuan *et al*., 2008; Figure 2).

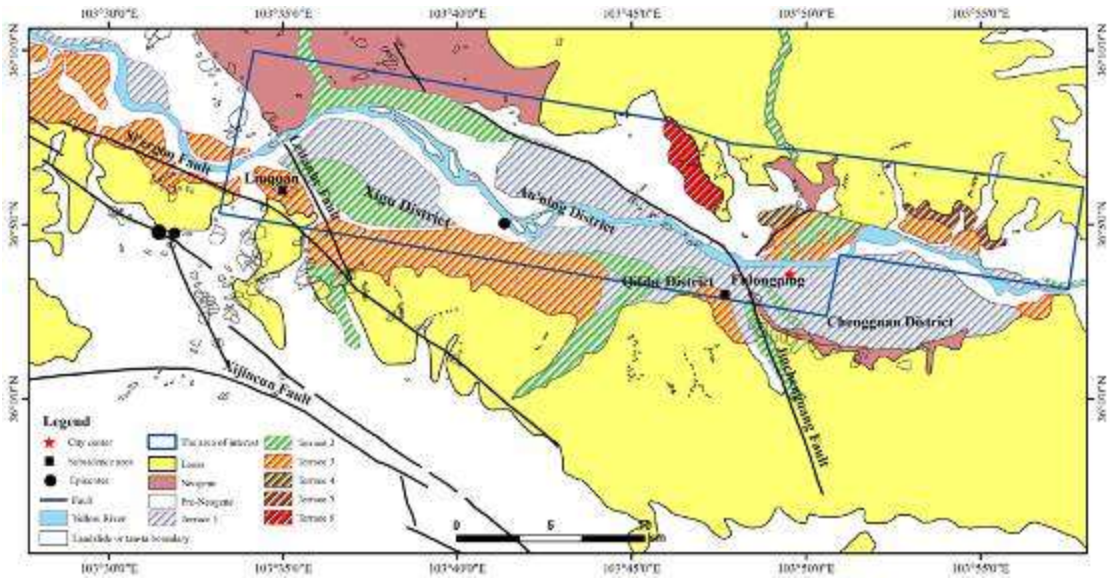


**Figure 2.** Geological sketch map of the Lanzhou area. The area of interest covers some 283 km$^2$, largely covering the greater Lanzhou urban region, with elevations ranging from 1500 m to 2100 m. The black polygons represent the locations of landslides and tan-ta (clusters of small failures in loess deposits).

The city of Lanzhou houses some 2 million people in an area of approximately 180 km$^2$ (Ding & Li, 2009). For most of the city, the population density exceeds 10,000 people per km$^2$. Recent population growth and industrial development have been dramatic, as illustrated by the doubling of the GDP in ten years. However, the mountainous regions around the city impose great constraints on the space available for urban growth and further development of transport systems. The lower terraces of the Yellow River have already been used close to their full capacity for building purposes, and construction has encroached on landforms such as the higher Yellow River terraces, tributary valleys, ancient landslide bodies, alluvial fans, and debris flow deposits. Where construction and land-use practices do not recognise the inherent instability of this landscape, invariably the consequences are severe resulting in, at least, significant economic impacts and, at worst, loss of life (Derbyshire *et al.*, 2000, Dijkstra *et al.*, 2014).

The area of interest focused on the greater Lanzhou urban region where most development is taking place, i.e. the districts of Xigu, An'ning, Qilihe and the terrace areas north of the Yellow River in the Chengguan District of eastern Lanzhou. Ground deformation in these urban regions continues to pose a problem and the PS-InSAR technique offers a unique opportunity to monitor the degree of ground motion and evaluate the possible consequences.

## 3. Factors influencing ground instability in the Lanzhou region

Case study analyses (including those reported by Derbyshire *et al*., 2000; and site investigations carried out by the authors) concluded that, in addition to the effects of human interference in this terrain, several major factors contribute to the susceptibility of the terrain in this region to generate ground instability. The following sections provide brief descriptions of the main influencing parameters.

**Loess**

The Lanzhou region can be broadly characterized by an undulating surface of pre-Pleistocene bedrock on top of which a widespread, thick loess deposit is found of predominantly Pleistocene age (with a thin Holocene drape in many places). The distribution of loess is of greatest importance for the determination of the potential instabilities in this landscape. Research indicates that where loess becomes relatively thin the type of bedrock starts to play an important role in contributing to slope instability processes (Derbyshire *et al*., 2000).

The Lanzhou loess is subdivided into four main units Wucheng (early Pleistocene), Lishi (mid Pleistocene), Malan (late Pleistocene) and Holocene loess. Malan and Holocene loess are much more weakly cemented, and contain many macro-pores and thus are much more susceptible to fabric collapse (upon wetting or shear) and ground deformation processes. The older loess units (Wucheng and Lishi) are strongly cemented and have relatively low void ratios resulting in a low collapsibility potential. Lishi and Wucheng loess materials are significantly stronger, rock-like materials when undisturbed (Wang et al., 1994; Derbyshire *et al*., 2000; Wu & Zhao2001).

The natural moisture content of Lanzhou loess is generally low (between 8 to 10% by weight), but upon wetting this low plasticity material has the potential to rapidly transform into a slurry. Some physical characteristics of Lanzhou loess are shown in Table 1.

**Table 1.** Characteristic properties of Lanzhou loess (after Wang *et al*., 1994; Derbyshire *et al*., 2000).

| **Parameters** | **Malan loess** | **Lishi loess** | **Wucheng loess** |
|---|---|---|---|
| age | Late Pleistocene | Mid-Pleistocene | Early Pleistocene |
| bulk density ($Mg/m^3$) | 1.38 | 1.57 | 1.72 |
| in situ moisture content (%) | 5.0 | 7.8 | 7.5 |
| porosity (%) | 52 | 47 | 43 |
| degree of saturation | 15.6 | 23.5 | 29.2 |
| liquid limit(%) | 29 | 28 | 28 |
| plastic limit(%) | 19 | 19 | 19 |
| plasticity index | 10 | 9 | 9 |
| cementation shear strength ($kN/m^2$) | 60-150 | 85-400 | $150\text{-}400^+$ |
| residual cohesion ($kN/m^2$) | 6-10 | 8-15 | 9-21 |
| angle of internal friction (degrees) | 25-33 | 27-32 | 27-35 |

**Geomorphology**

The terrain unit forms a convenient parameter to reflect different landforms characterising the geomorphology of the Lanzhou region. In broad terms, three main geomorphological entities can be observed; fluvial landforms of the Yellow River, long ridges formed in thick loess ('*liang*' in Chinese), and mountainous terrain that is mainly controlled by bedrock (Figure3). Where drapes of relatively young loess deposits (particularly Malan and Holocene loess) are found, ground instability in the form of subsidence/collapse and landslides is common. This is particularly the case for terrace levels 3 and 4 and throughout the loess ridge landscapes (Derbyshire *et al*., 2000).

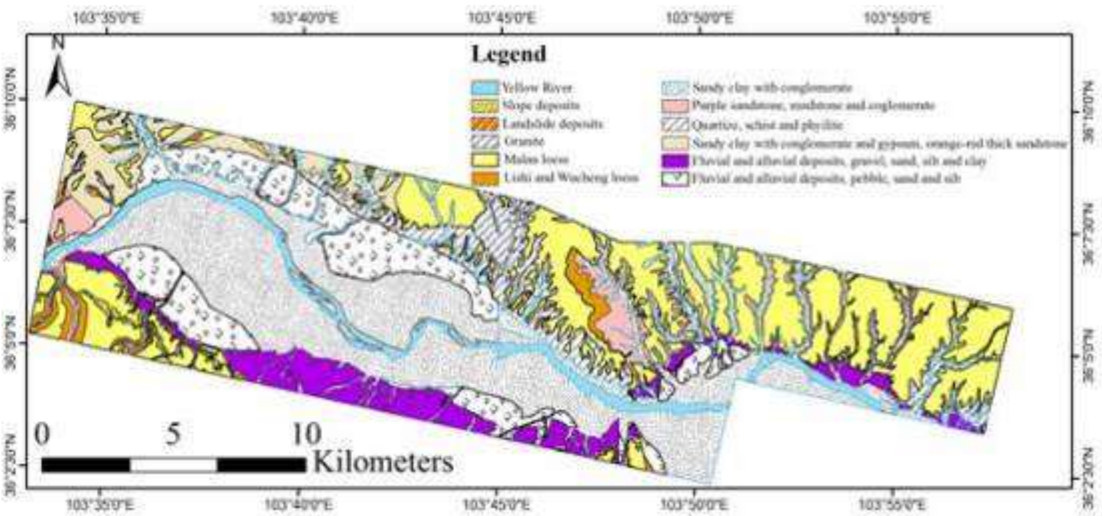


**Figure 3.** Litho-stratigraphical sketch map of the Lanzhou area.

*Fluvial landforms of the Yellow River*

In addition to the current active floodplain, six fluvial terrace levels of the Yellow River are recognised in the Lanzhou area. These terraces generally comprise a planated bedrock surface that is covered by fluvial deposits (ranging in thickness from 2 to 8 m) and a suite of loess deposits ranging in thickness from just a few metres to more than 300 m, but substantial loess thickness only occurs on the oldest three terrace levels (Figure 4). The fluvial deposits range in material from clayey silts to coarse gravels (Figure 3).

Most of the urban and industrial zones of Lanzhou are located on Terrace levels 1 and 2 (positioned some 6 and 14 m above the current river level). Terrace levels 3 and 4 are approximately 35 and 75 m above the Yellow River and are strongly affected by construction of terraces for agriculture, slope cuts and irrigated land-use, with occasional small developments associated with urban expansion. Terrace levels 5 and 6 are found some 140 and 250 m higher than the Yellow River and only in very few places are affected by construction (Table 2, Figure 4).

**Table 2.** Relative elevation and characteristic loess cover thickness of palaeo-terraces of the Yellow River. See Figure 4 for a schematic litho-stratigraphical cross section.

| Terrace number | Elevation above present Yellow River level （m） | characteristic loess thickness(m) |
|---|---|---|
| 1 | 6-8 | 4-7 |
| 2 | 12-14 | 10 |
| 3 | 35 | 15 |

| | | |
|---|---|---|
| 4 | 75 | 75 |
| 5 | 140-150 | 180 |
| 6 | 200-250 | 300 |

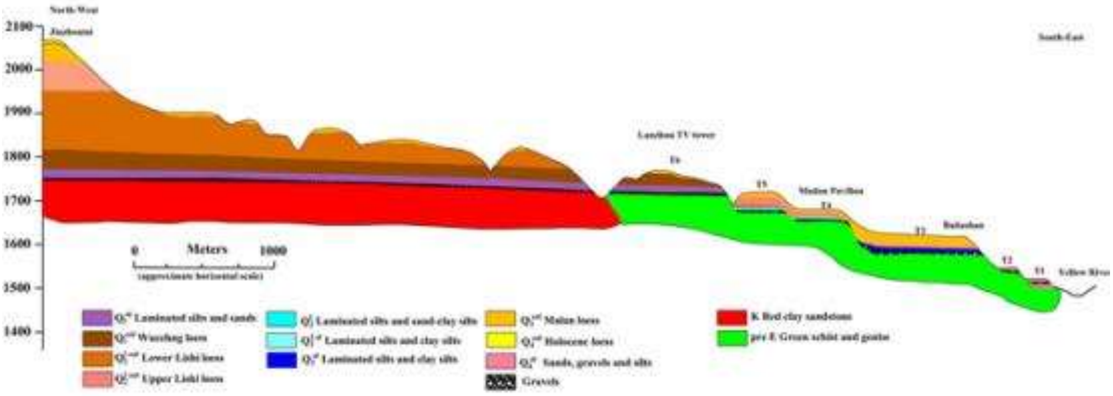


**Figure 4**. Schematic cross section of loess covered Yellow River palaeo-terraces (after Derbyshire *et al.*, 2000).

*Long ridges formed in loess (liang)*

The long ridges formed in thick loess deposits are found in a transitional zone between the Yellow River and the bedrock-controlled mountains to the south. This zone is some 5 to 10 km wide in the western part of the Lanzhou region, increasing in width to about 15 km in the east. The morphology is characterised by a series of parallel ridges separated by deep, narrow and steep-sided valleys. The maximum altitude of the ridges ranges from 1840 to 2200 m and average slope angles generally exceed 35 degrees. The relative relief is of the order of 400 to 500 m. Loess thickness is approximately 150 m with many loess slopes being close to equilibrium requiring only a small trigger to cause widespread slope failures.

*Bedrock controlled mountainous terrain*

Areas of widespread bedrock outcrops are confined to the mountainous zones south of Lanzhou city, notably in the Qidaoliang Mountain (elevations of 2300 - 2500 m). Here, relative relief is 200 - 400 m and the valleys are narrow and V-shaped.

**Geology**

In Lanzhou, the bedrock, in many places underlying thick loess deposits, consists of three types: Ordovician gneiss and shale, Cretaceous argillites and arenites, and Neogene argillites containing some sandy layers (Figures 2 and 3). The Ordovician rocks are exposed in the western part of the loess ridge area, the Cretaceous rocks are found between the Xuanjia and Hou valleys, while the Neogene outcrops mainly between Gaolan Mountain and the Lanni valley. In the mountains south of Lanzhou, the bedrock consists mainly of Precambrian and Ordovician metamorphic rocks and basalts, andesitic tuffs, gneiss, shales and granite.

The Lanzhou region is positioned in the northeast extension zone of the tectonically active Tibetan plateau (Dijkstra *et al*., 1993; Derbyshire *et al*., 2000) and has been suffering from intermittent periods of uplift since at least the early Quaternary. The total uplift for this period is estimated at some 250 m, based the height and age of the oldest terrace of the Yellow River (formed about 2.4 Ma BP; Derbyshire &Mellors, 1988). Much of the tectonic stress release occurs along systems of strike slip faults. Seismic refraction, a drilling campaign and observations from large trenches have confirmed the existence of four large active Pre-Quaternary fault zones (Yuan *et al*., 2008; Figure 2). The Jinchengguan and Xijincun fault zones have a general WNW strike direction that coincides with the regional stress field. The Leitanhe and the Si'ergou fault zones follow a NNW alignment and influence the direction of many valleys and fault depressions. Earthquakes generated along these faults can trigger widespread ground instability and in the Lanzhou region there is widespread evidence of ancient landslides that provide an insight into landscape adjustment to neotectonic deformations. Many valleys have responded to the phases of uplift (and associated relative lowering of the erosion base) are shaped like a V and are narrow and deep. Valleys with more gentle slope profiles are also found and these occur where (a) adjustment of erosion base lowering has not yet taken place (high in the mountains, or close to the top of the valleys between the loess ridges), or (b) valley incision has progressed to find an equilibrium with the regional erosion base.

**Slope aspect and vegetation cover**

Dependent on aspect, slopes receive variable amounts of solar radiation that affect soil moisture content and surface vegetation. Soil moisture directly affects the amount of shear strength that can be mobilized in loess (Dijkstra,2000). Vegetation has a complex relationship with ground stability in this region. Root strength can provide additional shear strength and erosion resistance, but root action can also affect loess structure so that is loses cemented strength in the process and becomes much weaker as a result. Lanzhou is situated in a semi-arid environment with a large surplus of potential evapotranspiration. To promote vegetation growth (whether for agriculture or reforestation) many loess slopes in the Lanzhou urban region are irrigated and this has resulted in higher soil moisture levels and elevated water tables. This affects the structural stability of loess and can lead to ground instability, such as ground subsidence and slope instability.

To illustrate the distribution of vegetation in the Lanzhou region a vegetation cover index was extracted from Landsat-5 images using bands 3 and 4. A high vegetation index (greater than 0.6), indicative of a lush cover of shrubs and trees, is found where afforestation is supported through intensive irrigation (for example, on the slopes of temple complex of Baita Shan (Figure 5)).However, the majority of the region is dominated by cover indices less than 0.5, indicative of a marginal cover of mainly shrubs and grasses (Figure 5).

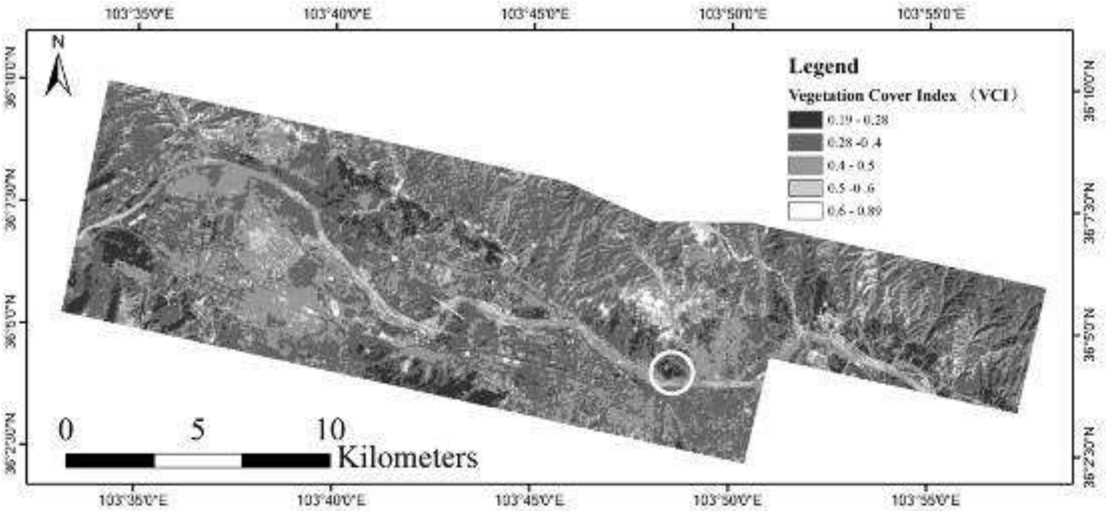


**Figure 5.** Vegetation cover index map of the Lanzhou area as extracted from the Landsat-5images acquired in September, 2010. The data set is provided by Geospatial Data Cloud, Computer Network Information Center, Chinese Academy of Sciences. (http://www.gscloud.cn). Baita Shan is located inside the white circle.

## 4 Synthetic Aperture Radar Interferometry in the Lanzhou region

InSAR (Synthetic Aperture Radar Interferometry) was firstly designed to map the surface of the earth, and it can be used to study atmosphere (Hanssen *et al*., 1999), vegetation coverage (Askne *et al*., 1997; Hagberg *et al*., 1995; Treuhaft *et al*., 1996; Wegmuller& Werner, 1997; Strozzi *et al*., 2000) and ground deformation (Massonnet *et al*., 1993; Rott *et al*., 1999). The use of space-borne SAR imagery and differential interferometry (D-InSAR) to detect sub-centimeter of the Earth's surface started in the late 1980s (Gabriel *et al*., 1989). D-InSAR has a high measurement spatial resolution, large area coverage, all time and all weather detection advantage, and thus has been used widely by earth scientists (Peltzer & Rosen, 1995; Buergmann *et al*., 2000; Catani *et al*., 2005; Yang *et al*., 2010; Han *et al*., 2010). Although D-InSAR has great potential in wide-area ground deformation detection, and has also achieved some successful results, it cannot precisely monitor single targets. In addition, temporal and geometrical de-correlation (Rodriguez & Martin, 1992; Zebker & Villasenor, 1994) and the temporal and spatial changes in the atmospheric content (Goldstein, 1995) can prevent D-InSAR from being an operational tool for ground deformation monitoring. These limitations can be overcome to some extent by applying multi-temporal interferometry techniques based on Permanent Scatterers (PS-InSAR; Ferretti *et al*., 2001). This and similar advanced processing techniques are able to filter out the atmospheric noise through a multi-temporal analysis which detects targets, known as Persistent Scatterers (PS), showing high temporal and geometric radar signal stability.

Multi-temporal interferometry techniques have been used in the monitoring and mapping of landslides (Colesanti *et al*., 2003; Farina *et al*., 2006; Colesanti & Wasowski, 2006; Cigna *et al.,* 2013a; Bianchini *et al.,*2012, Bovenga *et al.,*2012, Hoelbling *et al.,* 2012, Cigna *et al.,* 2013b, Bovenga *et al.,* 2013), surface subsidence (Hooper *et al*., 2007; Heleno *et al*., 2011; Osmanoglu *et al*., 2011; Hung *et al*.,2011), active faults (Dehls *et al*., 2002; Sousa *et al*., 2010), mine subsidence (Jung *et al*., 2007), and volcano activity (Hooper *et al*., 2004). For more background information on multi-temporal interferometry and its applications in slope and ground instability investigations the interested reader is referred to a review article by Wasowski and Bovenga (2014).

**Radar data processing**

The Lanzhou area of interest covers large and important areas of terrain that are not directly affected by construction, but are likely to generate ground instability that may affect urban developments. Therefore, the SPINUA (Stable Point Interferometry over Unurbanized Areas) algorithm has been used to process the radar data. The algorithm follows a PS-InSAR processing strategy optimised for detection and monitoring targets in non- or scarcely-urbanized areas (Bovenga *et al.,* 2005, 2006, 2012). SPINUA has been successfully applied to study landslides, subsidence processes and post-seismic deformations, and validated by using *in situ* measurements from both GPS/GNSS (Global Positioning System/Global Navigation Satellite System) and levelling (Reale *et al*., 2011; Bovenga *et al*., 2013).

Data processing involved the use of 40 ENVISAT ASAR (Advanced Synthetic Aperture Radar) images acquired between 16/08/2003 and 27/03/2010 along descending passes (Track = 61) to obtain the ground displacement mean velocity values along the satellite line of sight (around 23° with respect to the vertical). PS-InSAR processing provided also refined estimate of the PS target elevation, thus leading to improved geocoding accuracy, which is within the radar image resolution cell.

The reliability of the obtained PS-InSAR measurements can be assessed in terms of temporal coherence, which is a number in between 0 and 1. In the present case, only pixels with a coherence greater than 0.75 were selected. This resulted in the selection of 141,720 PS within the area of interest that could be used for further processing. A further selection was made based on the location of the PS; in many urban areas and particularly in the southeast on terraces 1 and 2 of the Yellow River new construction is developing rapidly and PS in this region were discarded. The process for this selection involved the following steps; a) select high deformation rate PS (>5 mm/y) and identify these on Google Earth, b) select the points affected by construction and determine their GPS positions, c) use these positions in ArcGIS to construct buffer and d) populate these buffers with 0 value to exclude them from the analysis. Following this procedure, further processing was based on a subset of 88,930 PS where we are confident that deformation is not associated with construction activities (Figure 6).

Keeping in mind the precision of the PS measurements and the quality of the results, which is case specific (depending on the specific dataset of radar imagery, environmental characteristics of the study area), a conservative average annual displacement threshold of -2 to +2 mm/yr has been applied to distinguish between moving (deformation PS or DPS) and stable points (SPS).Therefore, the vast majority of radar targets detected on these stable surfaces are SPS.

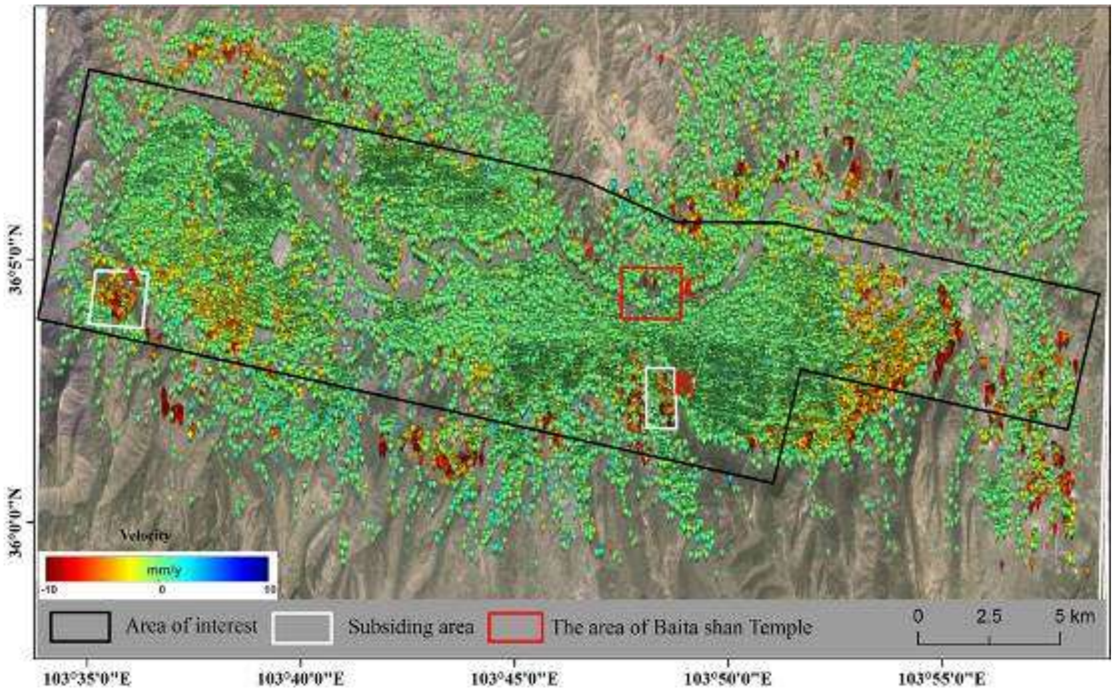


**Figure 6.** The distribution of PS results in the Lanzhou area. The subsiding area to the west (A) represents the conditions in the village of Liquan (see Figure 8 for further detail). The subsiding area in the centre (B) represents conditions in the district of Fulongping (see Figure 9 for further detail). (C) The red box indicates the location of slope failures in the Baita Shan area of central Lanzhou (see Figure 10 for further detail).

**Distribution of PS results**

Throughout the area of interest, a large number of PS was captured (based on Google Earth images) showing a good distribution of PS densities ranging from 50 to 350 targets per $km^2$ (Figure 6). Following comparison with the main units of the geological sketch map of Figure 2 it is apparent that the Holocene fluvial and alluvial deposits, and Yellow River terrace level 1 have very high densities (719 and 555 targets per $km^2$) as these are the classes where most built-up areas are found providing good, but stable radar targets. However, there are relatively fewer PS located on polygons identified as landslides in the area (only 512). This is related in part to the limited number of radar targets (typically buildings) in areas prone to these geohazards and where controls are in place to prohibit construction. In addition, the opportunities for capturing deformation associated with landslide activity in loess materials is limited. The method is best suited for those ground surface movements that are relatively slow, but frequent. Intact loess has significant cemented strength, generally failing in brittle mode. Therefore, pre-failure strains are generally very small, can be observed only over a short period of time and are therefore difficult to pick up with this method. Once a landslide has occurred a new, more stable state is generally achieved where further small strains are not significant. Pre-failure strains that are sufficiently large and occur over a sufficiently long period to be identified by PS-InSAR generally only apply to very large landslides in thick loess deposits (> 1 million cubic metres and with loess thickness exceeding some 100 m; see *e.g*. Dijkstra, 2000).

**Field investigations of areas of extensive ground deformation**

Where local clusters of deformation are identified it provides an important indication that a potential problem may exist involving ground instability. This thus warrants further investigation. For several key areas the observed PS values were checked using GPS. Where movement was caused by settlement (due to recent building construction), PS observation are classified as 'false' (thus turning a DPS into a SPS), and A 'true' classification is returned where the observed PS are located in zones of ground deformation (Figure 7).

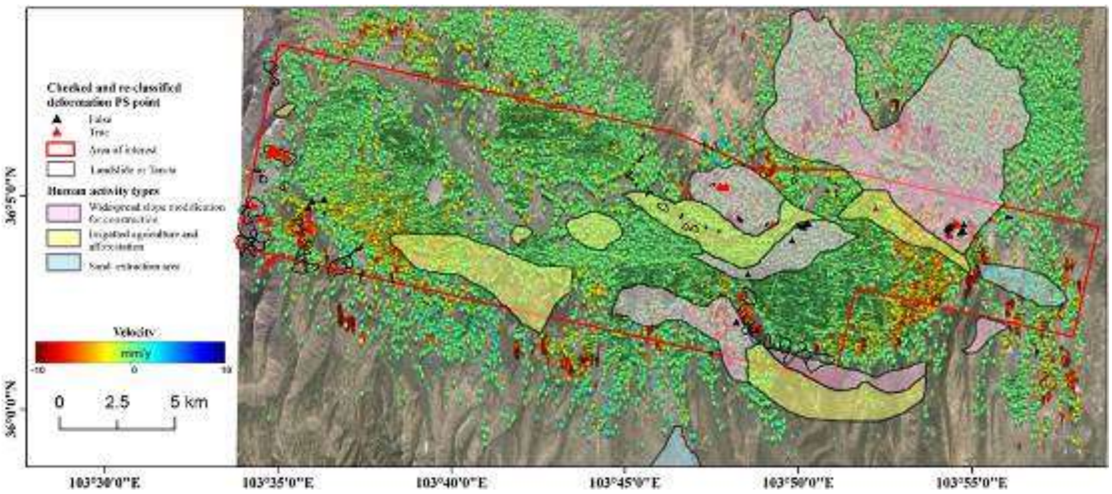


**Figure 7**. Land-use and landslide map of the Lanzhou area with an indication of PS indicators of ground movement. For a sub-set of these PS ground truth was carried out using GPS. Further field investigations at Liquan, Fulongping, and Baita Shan clarified the probable cause of ground deformation (black dots represent deformation caused by human activities, such as building/removal of structures, red dots represent ground instability). The black polygons represent the locations of landslides and tan-ta (clusters of small failures in loess deposits).

On the basis of the distribution of PS points throughout the area of interest, three areas were identified for further field investigation; the village of Liuquan (Polygon A in Figure 6), the district of Fulongping (Polygon B in Figure 6), and the area around Baita Shan (Polygon C in Figure 6).

The PS density for Liuquan was 510 PS/km$^2$ and for Fulongping a density of 986 PS/km$^2$ was achieved, providing ample density of information regarding ground movement based on a large number of PS where significant (i.e. greater than 2mm/year) deformation was observed. In the Baita Shan area a PS density of 145 PS/km$^2$ was achieved, but significant ground deformation was indicated in only a few places, at times just as single DPS surrounded by SPS.

In Liuquan (Figure 8) ground movement in the western part of the village was previously unknown. This village is situated on top of the 3$^{rd}$ terrace of the Yellow River that, in turn, is covered by a substantial thickness of Malan loess (more than 20 m). There are clear concentrations of PS points indicating annual deformations of more than 2 mm/year resulting in cumulative deformations measuring some 10 to 30 mm over the period 2003 to 2010 (Wasowski *et al*., 2011). Alignment and clustering gave rise to some concern as to what processes could be causing these patterns of deformation. During the field inspection, it became clear that the main mechanism causing the ground to subside was related to the position of poorly functioning drains. Water leaking from these conduits changed the moisture content of the Malan loess leading to a progressive collapse of the fabric that in turn was transferred through structural deformations of the surrounding buildings picked up by the PS-InSAR analysis.

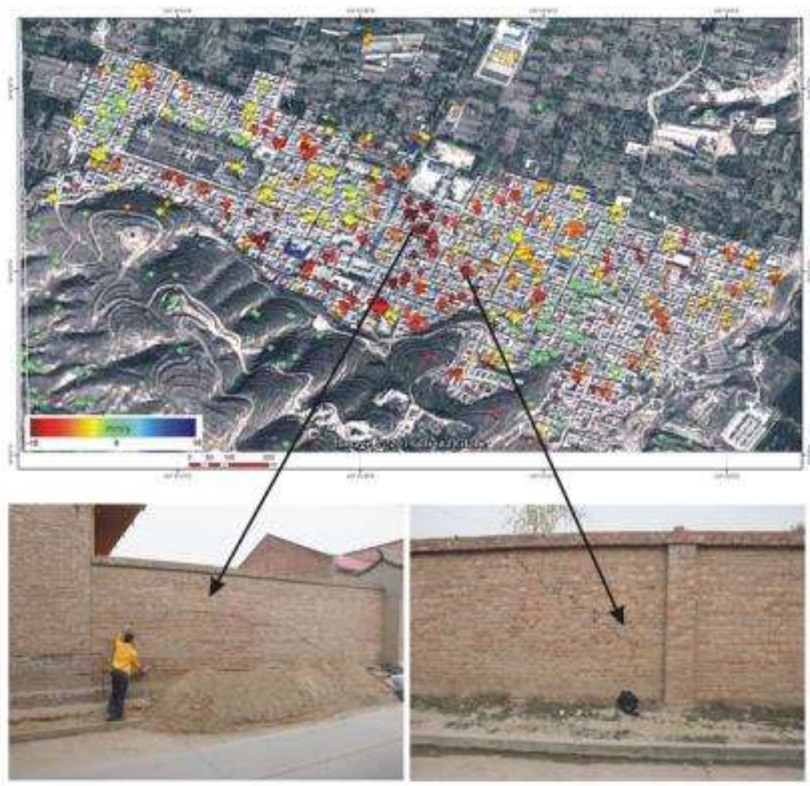

**Figure 8.** The PS results for the village of Liuquan. This village is located on the 4th river terrace, which is covered by thick Malan loess. During field investigations evidence of ground/structural deformation was observed at many places where PS values showed high levels of deformation. For location in the Lanzhou study area see Figure 6.

**Figure 9.**The PS results for the district of Fulongping and an example of structural deformation due to ground movement as observed during field investigation. For location in the Lanzhou study area see Figure 6.

In the district of Fulongping, loess collapse phenomena were well known as the cause of considerable damage to buildings (Figure 9). Again, most damage occurs to buildings in this area that are located on the 3rd river terrace where local thicknesses of Malan loess range from 20 to 55 m. Water entering the slopes (either through cracked pipes and drains, or through ingress of rainfall or irrigation water) poses a great risk to the stability of these collapsible loess deposits. Fieldwork confirmed that the PS correctly indicated areas where ground deformation is causing serious issues for construction.

The area around the Baita Shan temple complex in central Lanzhou is known to be affected by unstable ground (Figure 10). On these steep slopes on the lower flanks of Jiuzhoutai mountain substantial changes have taken place during the target period of 2003 – 2010. These are in the form of changes in surface morphology due to widespread construction mainly involving cut and fill operations to create terraces and provide footprints for infrastructure and new buildings. However, important changes are also taking place within these loess deposits. In this area intensive irrigation is practiced to support afforestation of these slopes and this changes the groundwater regime. Greater availability of soil moisture can lead to the collapse of loess fabrics, and the formation of extensive tunnel and pipe networks (loess pseudokarst; Figure 10).

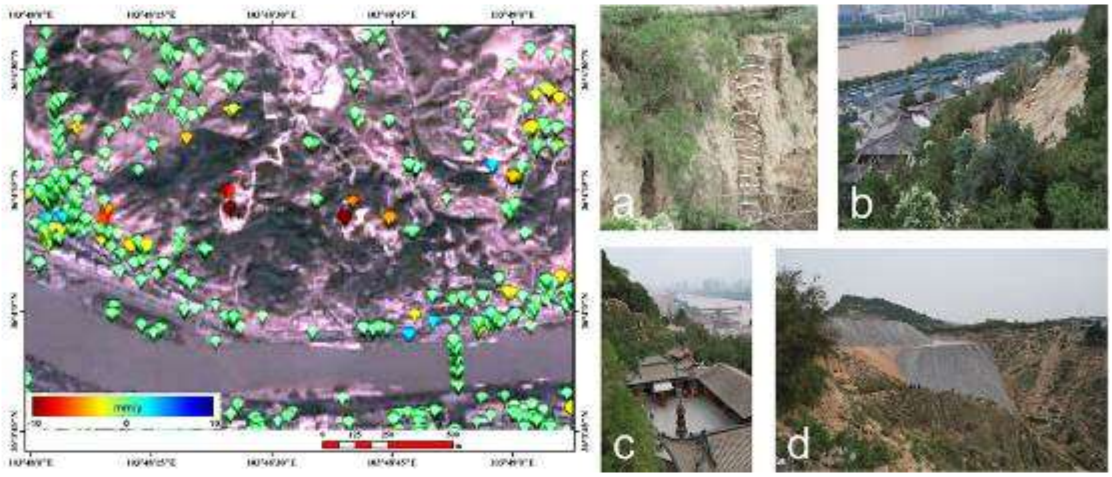


**Figure 10.**The PS results for the Baita Shan area and (a) examples of piping in loess and partial remediation through infill;(b) small scale landsliding; (c) and slope reinforcement to protect infrastructure and construction; and (d) valley infills as observed during field investigation. For location in the Lanzhou study area see Figure 6.

## 5 Conclusions

The application of the PS-InSAR technique in the Lanzhou Basin confirms its capability for detecting and mapping ground deformation at sub-regional and local scales, a technique that,in synergy with field investigations verifying local influencing conditions of geology, geomorphology, land use and construction, offers great advantages for planning and hazard management in this meta-stable terrain. The interpretation of the interferometry results, in terms of temporal evolution of the ground deformation, is limited by the lack of ground control data (e.g. inclinometer, topographic surveys) for the period of radar data acquisition (2003-2010) and this will be the subject of planned future research, which includes detailed investigations of the influence of human activity on geohazards.

Few permanent scatterers are located on mapped landslides in the Lanzhou region. This is not unexpected as pre-failure strains in loess are very small. Nevertheless, where strains are measured it is prudent to use these as indicators for potential ground instability and plan further field investigations. The interferometric patterns shown as overlays on maps or satellite imagery can quickly highlight targets for further checking and can focus attention to sites of special concern. However, to enable capture of pre-failure strains, image sequences with short time intervals (several per year) need to be considered.

The approach is most suited to detecting spatially distributed, gradual deformation processes in loess and has shown its greatest value in areas where, due to poor drainage, extensive ground deformation occurs due to structural collapse of Malan and Holocene loess deposits. In these cases, it can therefore form a suitable monitoring approach.

The PS-InSAR results highlights that, in particular, the higher terrace levels of the Yellow River are prone to ground instability in this sensitive environment. There are indications that the stability of these terraces depends on their recent development history and land use, in particular when irrigation or poor drainage is involved.

In this densely populated city, the consequences of ground instability can be severe. It is therefore imperative that both construction and irrigation practices are managed sensitively in the meta-stable loess landscape. Inappropriate drainage, or complete lack thereof, will result in long-term consequences for ongoing ground deformation, not just on the river terraces as identified in this study, but also elsewhere in the Lanzhou region where new construction continues to involve large scale landscape reconstruction filling in valleys without due consideration for appropriate drainage in, or long term volume stability of reworked loess deposits (Dijkstra *et al*., 2014; Li *et al*., 2014). In due course, these new construction areas are therefore expected to generate further interesting case studies for the application of PS-InSAR.

## Acknowledgements

This research was supported by the National Natural Science Foundation of China (NO. 41172328), the Natural Science Foundation of Gansu Province (NO.1107RJZA093), the National Major State Basic Research Development Program (973 Program, NO.2014CB744703) and the Fundamental Research Funds for the Central Universities (NO.lzujbky-2014-267). The ENVISAT images were provided by ESA in the framework of CAT-1 project #7444 Exploitation of ENVISAT radar data for ground and infrastructure instability hazard assessments in the Lanzhou area (Gansu Province, China) and radar data processing was done by GAPsrl. We also thank Emily Derbyshire for her assistance with early drafts of the manuscript, and Chen Guan, Guo Peng, GuoJianjun, Zhang Yi, Qiao Liang and Li Yajun who helped in the field reconnaissance.

## References

Askne, J.I., Dammert, P.B.,Ulander, L.M. & Smith, G., 1997.C-band repeat-pass interferometric SAR observations of the forest. Geoscience and Remote Sensing, IEEE Transactions on, 35, 25-35.

Bianchini, S., Cigna, F., Righini, G., Proietti, C. & Casagli, N., 2012. Landslide HotSpot Mapping by means of Persistent Scatterer Interferometry. Environmental Earth Sciences, 67, 1155-1172.

Bovenga, F., Refice, A., Nutricato, R., Guerriero, L. & Chiaradia, M.T., 2005.SPINUA: a flexible processing chain for ERS / ENVISAT long term Interferometry. Proceedings of ESA-ENVISAT Symposium,September 6-10, 2004, Salzburg, Austria.ESA Special Publication SP-572, April 2005, CD. ISBN 92-9092-883-2, ISSN 1609-042X.

Bovenga, F., Nutricato, R., Refice, A. & Wasowski, J., 2006.Application of Multi-temporal Differential

Interferometry to Slope Instability Detection in Urban/Peri-urban Areas. Engineering Geology, 88,218-239.

Bovenga F., Wasowski J., Nitti D.O., Nutricato R. & Chiaradia M.T., 2012.Using COSMO/SkyMed X-band and ENVISAT C-band SAR interferometry for landslides analysis. Remote Sensing of Environment, 119, 272-285.

Bovenga, F., Nitti, D. O., Fornaro, G., Radicioni, F., Stoppini, A. & Brigante, R., 2013. Using C/X-band SAR interferometry and GNSS measurements for the Assisi landslide analysis. International Journal of Remote Sensing, 34, 4083-4104.

Bürgmann, R., Rosen, P.A. & Fielding, E.J., 2000. Synthetic aperture radar interferometry to measure Earth's surface topography and its deformation. Annual Review of Earth and Planetary Sciences, 28, 169-209.

Catani, F., Farina, P., Moretti, S., Nico, G. & Strozzi, T., 2005. On the application of SAR interferometry to geomorphological studies: estimation of landform attributes and mass movements. Geomorphology, 66, 119-131.

Cigna, F., Bateson, L, Jordan, C. & Dashwood, C., 2013a. Nationwide monitoring of geohazards in Great Britain with InSAR: Feasibility mapping based on ERS-1/2 and ENVISAT imagery. IEEE International Geoscience and Remote Sensing Symposium (IGARSS), 672-675.

Cigna, F., Bianchini, S. & Casagli, N., 2013b. How to assess landslide activity and intensity with Persistent Scatterer Interferometry (PSI): the PSI-based matrix approach. Landslides, 10, 267-283.

Colesanti, C., Ferretti, A., Prati, C., & Rocca, F., 2003. Monitoring landslides and tectonic motions with the Permanent Scatterers Technique. Engineering Geology, 68, 3-14.

Colesanti, C. & Wasowski, J., 2006.Investigating landslides with space-borne Synthetic Aperture Radar (SAR) interferometry. Engineering Geology, 88, 173-199.

Dehls, J.F., Basilico, M. & Colesanti, C., 2002.Ground deformation monitoring in the Ranafjord area of Norway by means of the Permanent Scatterers technique. Geoscience and Remote Sensing Symposium.IGARSS'02.2002 IEEE International. IEEE, pp. 203-207.

Derbyshire, E. & Mellors, T., 1988. Geological and geotechnical characteristics of some loess and loessic soils from China and Britain: a comparison. Engineering Geology, 25, 135-175.

Derbyshire, E.D., Meng, X. & Dijkstra, T.A., 2000. Landslides in the thick loess terrain of North-West China. John Wiley & Sons Inc. pp: 23-42,173-202.

Dijkstra, T.A., 2000. Loess slope instability of the Lanzhou Region, China [D]. Utrecht: University of Utrecht. 308p.

Dijkstra, T.A., Derbyshire, E. & Meng, X.M., 1993. Neotectonics and mass movements in the loess of north-central China. In: L.A. Owen, I. Stewart, C. Vita-Finzi (Eds.),Neotectonics: Recent advances, Quaternary Proceedings, 3, pp: 93–110.

Dijkstra T.A., Rogers C.D.F., Smalley I.J., Derbyshire E., Li Y.J. & Meng X.M., 1994. The loess of north-central China: Geotechnical properties and their relation to slope stability. Engineering Geology, 36, 153 - 171.

Dijkstra, T.A., Wasowski, J., Winter, M.G. & Meng, X.M., 2014. Introduction to Geohazards in Central China. Quarterly Journal of Engineering Geology and Hydrogeology, on-line first, first published on July 31, 2014, doi:10.1144/qjegh2014-054

Ding, Z.Q.& Li, Zh.H., 2009. The prevention and control of geohazards in Lanzhou City. Lanzhou: The Gansu Province Science and Technology Press, pp: 8-10, 54-62.

Farina, P., Colombo, D., Fumagalli, A., Marks, F. & Moretti, S.,2006.Permanent Scatterers for landslide investigations: outcomes from the ESA-SLAM project. Engineering Geology, 88, 200-217.

Ferretti, A., Prati, C. & Rocca, F., 2001.Permanent Scatterers in SAR interferometry. Geoscience and Remote Sensing, IEEE Transactions on, 39, 8-20.

Gabriel, A.K., Goldstein, R.M. & Zebker, H.A., 1989. Mapping small elevation changes over large areas: Differential radar interferometry. Journal of Geophysical Research, 94, 9183-9191.

Goldstein, R., 1995. Atmospheric limitations to repeat-track radar interferometry. Geophysical Research Letters, 22, 2517-2520.

Hagberg, J.O., Ulander, L.M. & Askne, J., 1995.Repeat-pass SAR interferometry over forested terrain.Geoscience and Remote Sensing, IEEE Transactions on, 33, 331-340.

Han, Y.F., Song, X.G., Shan, X.J., Qu, C.Y., Wang, C.S., Guo, L.M., Zhang, G.F. & Liu, Y.H., 2010.Deformation monitoring of Changbaishan Tianchi volcano using D-InSAR technique and error analysis. Chinese Journal of Geophysics (in Chinese), 53, 1571-1579.

Hanssen, R.F., Weckwerth, T.M., Zebker, H.A. & Klees, R., 1999.High-resolution water vapor mapping from interferometric radar measurements. Science, 283, 1297-1299.

Heleno, S.I., Oliveira, L.G., Henriques, M.J., Falcão, A.P., Lima, J.N., Cooksley, G., Ferretti, A., Fonseca, A.M., Lobo-Ferreira, J.P. & Fonseca, J.F., 2011. Persistent Scatterers Interferometry detects and measures ground subsidence in Lisbon. Remote Sensing of Environment, 115, 2152-2167.

Hölbling, D.,Füreder, P., Antolini, F., Cigna, F., Casagli, N. & Lang, S., 2012. A semi-automated object-based approach for landslide detection validated by Persistent Scatterer Interferometry measures and landslide inventories. Remote Sensing, 4, 1310-1336.

Hooper, A., Zebker, H., Segall, P. & Kampes, B., 2004.A new method for measuring deformation on volcanoes and other natural terrains using InSAR persistent scatterers. Geophysical Research Letters, 31, 611-615.

Hooper, A., Segall, P. & Zebker, H., 2007.Persistent scatterer interferometric synthetic aperture radar for crustal deformation analysis, with application to VolcánAlcedo, Galápagos.Journal of Geophysical Research, 112(B7), B07407. 21p.

Hung, W.C., Hwang, C., Chen, Y.-A., Chang, C.P., Yen, J.Y., Hooper, A. & Yang, C.Y., 2011. Surface deformation from Persistent Scatterers SAR Interferometry and fusion with leveling data: A case study over the Choushui River Alluvial Fan, Taiwan. Remote Sensing of Environment, 115, 957-967.

Jung, H.C., Kim, S.W., Jung, H.S., Min, K.D. & Won, J.S., 2007.Satellite observation of coal mining subsidence by persistent scatterer analysis. Engineering Geology, 92, 1-13.

Li, S., Wang, Y., Chen, H.Z. & Yan, M.C., 1993. Neo-tectonics of the Yellow River Valley in Lanzhou.Geological Review (in Chinese), 39, 259-267.

Li, P.Y., Qian, H. & Wu J.H., 2014. Environment: Accelerate research on land creation. Nature 510, 05 June 2014, pp: 29–31

Massonnet, D., Rossi, M., Carmona, C., Adragna, F., Peltzer, G., Feigl, K. & Rabaute, T., 1993. The displacement field of the Landers earthquake mapped by radar interferometry. Nature, 364, 138-142.

Osmanoğlu, B., Dixon, T.H., Wdowinski, S., Cabral-Cano, E. & Jiang, Y., 2011. Mexico City subsidence observed with persistent scatterer InSAR. International Journal of Applied Earth Observation and

Geoinformation, 13, 1-12.

Peltzer, G. & Rosen, P., 1995. Surface displacement of the 17 May 1993 Eureka Valley, California, earthquake observed by SAR interferometry. Science, 1333-1336.

Rodriguez, E. & Martin, J., 1992. Theory and design of interferometric synthetic aperture radars. Radar and Signal Processing, IEE Proceedings F. IET, pp. 147-159.

Reale, D., Nitti, D. O., Peduto, D., Nutricato, R., Bovenga, F. & Fornaro, G., 2011. Post-seismic deformation monitoring with the COSMO/SKYMED constellation. IEEEGeoscience and Remote Sensing Letters, 8, 696-700.

Rott, H., Scheuchl, B. & Siegel, A., 1999.Monitoring very show slope movement by means of SAR Interferometry: a case study from a mass waste above a reservoir in the Otztal Alps, Austria. Geophysical Research Letters, 26, 1629-1632.

Sousa, J.J., Ruiz, A.M., Hanssen, R.F., Bastos, L., Gil, A.J., Galindo-Zaldívar, J. & Sanz de Galdeano, C., 2010. PS-InSAR processing methodologies in the detection of field surface deformation - Study of the Granada basin (Central Betic Cordilleras, southern Spain). Journal of Geodynamics, 49, 181-189.

Strozzi, T., Dammert, P.B., Wegmuller, U., Martinez, J.-M., Askne, J.I., Beaudoin, A. & Hallikainen, N., 2000.Land-use mapping with ERS SAR interferometry. Geoscience and Remote Sensing, IEEE Transactions on, 38, 766-775.

Treuhaft, R.N., Madsen, S.N., Moghaddam, M. & van Zyl, J.J., 1996.Vegetation characteristics and underlying topography from interferometric radar.Radio Science, 31, 1449-1485.

Wang, J.T., Li, Y.J. & Li, B.X., 1994. Physical characteristic of Lanzhou loess. Hydrogeology & Engineering Geology, China, 4, 12-17.

Wasowski, J. & Bovenga, F., 2014.Investigating landslides and unstable slopes with satellite Multi Temporal Interferometry: Current issues and future perspectives. Engineering Geology, 174, 103-138.

Wasowski, J., Bovenga, F., Nitti, D.O., Nutricato, R., Dijkstra, T. & Meng, X., 2011. PSI helps to map relative susceptibility to ground and slope instabilities in the Lanzhou loess area of Gansu Province, China. Proceedings of Fringe 2011 Workshop', Frascati, Italy, 19-23.

Wegmuller,U. & Werner, C., 1997.Retrieval of vegetation parameters with SAR interferometry.

Geoscience and Remote Sensing, IEEE Transactions on, 35, 18-24.

Wu, Y.P. & Zhao, C.X., 2001.The loessial geological property in Fulongping District of Lanzhou City. Journal of Gansu Science(in Chinese), 13,41-43.

Yang, C., Zhang, Q., Zhao, C.L. & Zhu, W. 2010. Monitoring mine collapse by D-InSAR. Mining Science and Technology (in Chinese), 20,696-700.

Yao, C.H., 2008. Study development model of urbanization & the level of forecasting Lanzhou[D] (in Chinese). Xi’an: Xi’an University of Technology. pp: 24.

Yuan, D.Y., Wang, L.M., He, W.G., Liu, B.C., Ge, W.P., Liu, X.W., Liang, M.J. & Zheng, W.J., 2008. New progress of seismic active fault prospecting in Lanzhou City. Seismology and Geology(in Chinese), 30, 236-249.

Zebker, H.A. & Villasenor, J., 1992.Decorrelation in interferometric radar echoes. Geoscience and Remote Sensing, IEEE Transactions on, 30, 950-959.